Long-Term Dispatch Method for Electro-Hydrogen Coupled Microgrids Considering a Tiered Carbon Trading Mechanism

Huiyu Miao[1], Xiaodong Yuan[1], Minghe Wu[2], Mingshen Wang[1], Yi Pan[1], Fei Zeng[1]
[1]Jiangsu Electric Power Research Institute Company Ltd., Nanjing 211100, China
[2]School of Electrical Engineering, Southeast University, Nanjing 210096, China

Corresponding author: Minghe Wu (e-mail: wu_mh@seu.edu.cn).

ABSTRACT Electro-hydrogen coupled microgrids (EHCMs), in which water electrolyzers, hydrogen fuel cells, and power-electronic converters act as cascaded electromagnetic–electrochemical energy conversion interfaces, significantly enhance the renewable energy hosting capacity and flexible regulation capability of distributed energy systems through cross-temporal energy conversion and dynamic power regulation. However, few studies have addressed the medium-to-long-term operational optimization of EHCMs under carbon trading mechanisms. This paper proposes a medium-to-long-term low-carbon economic dispatch framework for EHCMs incorporating a tiered carbon trading mechanism. First, a tiered carbon trading model based on hierarchical pricing is established, in which differentiated carbon price brackets strengthen the low-carbon dispatch incentives of EHCMs and maximize their emission reduction potential. Second, a typical-day scenario generation method based on spectral joint clustering is introduced; exploiting eigen-decomposition of the normalized graph Laplacian—a spectral analysis technique sharing its mathematical foundation with modal decomposition methods widely used in computational electromagnetics—the method preserves the key statistical and temporal characteristics of multi-energy time series while significantly reducing the dimensionality of the long-term optimization problem. Subsequently, a medium-to-long-term operational optimization model of EHCMs is constructed, comprehensively considering electricity, heat, natural-gas, and hydrogen balance constraints. With the objective of minimizing the annual operating cost, the model reveals cross-seasonal hydrogen storage operation strategies for electro-hydrogen coupled micro-energy networks. Case studies of a large-scale microgrid in Shanxi, China, verify the effectiveness of the proposed method in enhancing system economics and reducing carbon emissions.

INDEX TERMS Electro-Hydrogen Coupling, Electromagnetic Energy Conversion, Microgrid, Spectral Joint Clustering, Long-Term Optimization, Tiered Carbon Trading

I. INTRODUCTION

Under the influence of China's dual carbon policies, distributed renewable energy has developed rapidly. By the end of June 2024, China's cumulative installed capacity of distributed photovoltaic power had reached 310 gigawatts. Against this backdrop, energy storage as a flexible regulating resource effectively achieves peak shaving and valley filling while improving power quality, becoming a vital component for ensuring stable power system operation. Due to technical limitations and cost constraints, short-term storage technologies like lithium batteries struggle to address the long-duration energy imbalance challenges posed by distributed renewables. Consequently, exploring long-duration storage technologies capable of meeting cross-seasonal scheduling demands has emerged as a key research focus. Hydrogen storage not only provides flexible storage solutions for energy systems but also facilitates the coupling and interaction of different energy forms such as electricity, heat, and gas. electro-hydrogen coupled microgrids (EHCMs) achieve flexible conversion between electricity and hydrogen through processes like water electrolysis, high-pressure hydrogen storage, and fuel cells.

Reference [1] verifies the enhancement of economic and low-carbon benefits in distributed energy systems through medium-to-long-term hydrogen storage. Reference [2] proposes a microgrid configuration method incorporating electro-hydrogen hybrid storage, demonstrating the advantages of electro-hydrogen synergistic deployment in improving PV integration and voltage stability. Reference [3] introduces a power system security enhancement method considering electro-thermal-hydrogen conversion and seasonal hydrogen storage technology. Reference [4] employs nonlinear modeling to accurately describe the electro-hydrogen conversion process, thereby improving the modeling precision of distributed energy systems. However, existing studies often assume that the balancing time of hydrogen storage aligns with electrochemical storage, overlooking the unique advantages of hydrogen storage in cross-time-scale regulation, which limits its potential for long-duration energy storage and its ability to meet the demands for long-term and efficient system optimization.

In EHCMs, the role of hydrogen storage has expanded from a single energy storage solution to a multi-energy conversion hub. Reference [5] proposed an electro-hydrogen-carbon (E-H-C) coordinated economic dispatch model, integrating carbon capture technology to construct an energy flow model that achieves multi-energy complementarity. Reference [6] innovatively introduced a hydrogen-thermal multi-energy inertia model to optimize the operation of systems using hydrogen-blended natural gas. Reference [7] combined hydrogen storage, ammonia production, and carbon capture to create an "electric-hydrogen-ammonia" multi-energy chain, reducing carbon emissions by 21.21% in the park. Reference [8] developed a daily dispatch model for an integrated energy system consisting of power-to-hydrogen (P2H) and hydrogen storage, incorporating organic Rankine cycle waste heat recovery, and validated the synergy between economic and environmental goals. References [9]–[12] proposed various stochastic optimization methods to explore integrated optimization strategies for wind-solar-hydrogen systems, improving overall energy utilization. However, there is still insufficient research on the collaborative mechanisms of hydrogen energy with unique resources in EHCMs, such as biomass and biogas, and the waste heat recovery efficiency is limited by equipment costs and technological maturity.

To address the fluctuations in renewable energy and load uncertainties, various optimization strategies have been proposed. Reference [13] proposed a multi-objective optimization model for scheduling the uncertainty of renewable energy outputs. Reference [14] combined mixed-integer linear programming with battery storage to optimize electrolyzer operation strategies, balancing the economy and flexibility of wind-to-hydrogen systems. Reference [15] applied cooperative game theory and Shapley value allocation to reduce operational costs by 22.96% in collaborative scenarios. Reference [16] designed a two-stage scheduling model for hydrogen storage operation, reducing total load deviation by 14% through day-ahead economic optimization and intraday rolling correction. Reference [17] introduced day-ahead scheduling and real-time rolling optimization to coordinate energy storage, heating, and hydrogen storage devices. However, existing research on electro-hydrogen coupling systems has primarily focused on urban or industrial park scenarios, with insufficient consideration given to the load dispersion and seasonal characteristics of electro-hydrogen coupling micro-energy networks.

Carbon trading and low-carbon policies are key drivers for hydrogen energy storage applications. Reference [18] proposes an energy scheduling method for EHCMs that incorporates a master-slave game model and carbon trading mechanisms, achieving comprehensive improvements in both economic efficiency and low-carbon performance. Reference [19] explores optimized scheduling schemes for hydrogen energy storage within a carbon trading framework, demonstrating the role of carbon trading costs in integrated energy system scheduling. Reference [20] analyzes the operating costs of hydrogen storage under a tiered carbon trading mechanism and proposes an energy scheduling scheme for electro-hydrogen coupling systems based on model predictive control. Reference [21] introduces a tiered demand response and carbon trading mechanism, enhancing supply-side efficiency through waste heat recovery to reduce energy system operating costs. Reference [22] proposes a model predictive control strategy for distributed energy systems based on deep learning methods. However, existing carbon trading mechanisms remain confined to the framework of power system operations, failing to fully integrate the multi-energy complementary characteristics of electro-hydrogen coupled microgrids. Additionally, there is insufficient exploration of scheduling strategies for energy systems at medium-to-long-term scales.

Rural areas possess abundant wind and solar resources, yet their electricity load density remains extremely low. This necessitates urgent exploration of medium-to-long-term strategies for integrating new energy sources and developing hydrogen storage and utilization solutions. Reference [23] constructed a dynamic optimization model for rural areas by incorporating hydrogen energy storage. Reference [24] developed an integrated energy system optimization model encompassing photovoltaic hydrogen production, biogas fermentation, and energy storage for electricity-heat-cooling-gas applications. Reference [25] proposed an optimization method based on virtual energy storage to aggregate distributed loads, enhancing load management flexibility. Reference [26] established a cross-seasonal hydrogen storage model, enabling seasonal energy transfer through biomass integration. Reference [27] proposed a dynamic pricing model for shared energy storage, lowering the application threshold for hydrogen storage.

From the perspective of electromagnetic science and engineering, an EHCM is essentially a cascaded electromagnetic–electrochemical energy conversion system. Photovoltaic arrays, water electrolyzers, hydrogen fuel cells, and power-electronic converters are electromagnetic energy conversion devices whose efficiency characteristics, partial-load behavior, and dynamic constraints directly determine the feasible operating region of the microgrid. A long-term dispatch model therefore does more than minimize operating costs: it produces the operating-point envelopes, duty-cycle profiles, and cumulative energy-throughput spectra that are indispensable inputs for the electromagnetic design, thermal management, and lifetime assessment of these conversion devices. In addition, the typical-day generation method developed in this work is built upon eigen-decomposition of normalized Laplacian operators, a spectral analysis framework that shares its mathematical foundation with modal and spectral-domain techniques widely used in computational electromagnetics. Introducing this spectral technique into multi-energy time-series analysis establishes a methodological link between large-scale energy system optimization and the analytical and numerical techniques of interest to the electromagnetics community.

In summary, existing research primarily focuses on the short-term scheduling of EHCMs, with insufficient consideration of the long-duration operational characteristics of hydrogen storage, the seasonal fluctuations of loads and renewable generation, and the coupling between tiered carbon pricing and multi-energy coordination. To fill this gap, this paper proposes a medium-to-long-term low-carbon economic dispatch framework for EHCMs incorporating a tiered carbon trading mechanism. The main contributions are threefold:

(1) A tiered carbon trading model based on hierarchical pricing is formulated, in which differentiated carbon price brackets provide progressively stronger penalties for high-emission operation, thereby maximizing the emission reduction potential of EHCMs compared with flat carbon pricing.

(2) A typical-day scenario generation method based on spectral joint clustering is proposed. By performing eigen-decomposition on the normalized Laplacian matrices of both the temporal and feature dimensions, the method extracts representative daily scenarios that preserve the statistical characteristics, temporal correlations, and multi-energy coupling features of the original 8760-hour data, while reducing the dimensionality of the long-term optimization problem by nearly two orders of magnitude.

(3) A medium-to-long-term operational optimization model of EHCMs is constructed, integrating electricity, heat, natural-gas, and hydrogen balance constraints with a long-duration hydrogen storage operation model. Case studies validate the effectiveness of the synergy between long-duration hydrogen storage and tiered carbon trading in improving the economic and low-carbon performance of EHCMs, and the resulting operating-point envelopes provide quantitative inputs for the design and assessment of the electromagnetic energy conversion devices in EHCMs.

II. CARBON TRADING MECHANISM AND TYPICAL SCENARIO GENERATION METHOD FOR EHCMS

A. TIERED CARBON TRADING MECHANISM

The tiered carbon trading mechanism is an enhancement of traditional carbon market trading models, which primarily focuses on tiered carbon emission quantification. It establishes different tiers for carbon emissions, with each tier corresponding to an increased trading price. To quantify the carbon emissions of the EHCMs, the carbon emission baseline E_{base} needs to be defined as:

$$E_{\text{base}} = \sum_{i}^{Y} EF_i \times D_i. \tag{1}$$

Where, EF_i represents the emission strength of the i-th energy type in the electro-hydrogen coupled microgrid, and D_i is the carbon emission factor for the i-th energy type. The actual carbon emissions for the EHCMs are defined as:

$$E_{\text{actual}} = E_{\text{CP}} + E_{\text{AH}} + E_{\text{APP}} + E_{\text{buy}} - E_{\text{gar}} - E_{\text{BD}}. \tag{2}$$

Where E_{actual} represents the actual carbon emissions from the system. The difference between the actual emissions and the baseline is given by:

$$E_{\text{deal}} = E_{\text{actual}} - E_{\text{base}}. \tag{3}$$

The specific cost for different emission reductions can be expressed as:

$$C_{\text{CO2}} = \begin{cases} \lambda_{\text{CO2}} E_{\text{deal}}, & E_{\text{deal}} \le d, \\ \lambda_{\text{CO2}}(1+r)(E_{\text{deal}} - d) + \lambda_{\text{CO2}} d, & d \le E_{\text{deal}} \le 2d, \\ \lambda_{\text{CO2}}(1+2r)(E_{\text{deal}} - 2d) + \lambda_{\text{CO2}}(2+r)d, & 2d \le E_{\text{deal}} \le 3d, \\ \lambda_{\text{CO2}}(1+3r)(E_{\text{deal}} - 3d) + \lambda_{\text{CO2}}(3+3r)d, & 3d \le E_{\text{deal}} \le 4d, \\ \lambda_{\text{CO2}}(1+4r)(E_{\text{deal}} - 4d) + \lambda_{\text{CO2}}(4+6r)d, & 4d < E_{\text{deal}}. \end{cases} \tag{4}$$

Where C_{CO2} is the carbon trading cost for the EHCMs, λ_{CO2} is the unit price for carbon emissions, and d is the length of the emission reduction period, and r is the price increase rate. When E_{actual} is lower than E_{base}, the system can earn excess revenue from the carbon trading process.

B. EHCM CARBON TRADING MECHANISM AND TYPICAL SCENARIO GENERATION METHOD

1) TYPICAL SCENARIO GENERATION METHOD BASED ON SPECTRAL JOINT CLUSTERING

The main concept behind spectral joint clustering (SJC) is to improve the clustering of both rows and columns in a data matrix using matrix decomposition and spectral analysis. This approach helps identify the hidden relationships between variables and the time dimension. The mathematical framework is as follows:

Let the original data matrix be $\mathbf{X} \in \mathbb{R}^{m \times n}$, where m represents the number of days, and n represents the variables. Construct the corresponding similarity matrix $\mathbf{W}_r \in \mathbb{R}^{m \times m}$, which describes the similarity between the data for each day based on the variable vectors:

$$W_r(i,j) = \exp\left(-\frac{\|\mathbf{x}_i - \mathbf{x}_j\|^2}{2\sigma^2}\right). \tag{5}$$

Where $\mathbf{x}_i$ represents the feature vector of day i, and σ is the kernel bandwidth parameter that controls the rate of decrease in similarity.

Constructing a similarity matrix $\mathbf{W}_c \in \mathbb{R}^{n \times m}$, the similarity between small time slots can be expressed as:

$$W_c(k,l) = \exp\left(-\frac{\|\mathbf{x}_{:,k} - \mathbf{x}_{:,l}\|^2}{2\sigma^2}\right). \tag{6}$$

Where k and l are indices representing different time slots, $\mathbf{x}_{:,k}$ and $\mathbf{x}_{:,l}$ represent the k-th and l-th columns of the data matrix, respectively, indicating the data for all days corresponding to a specific variable at a particular hour.

For rows and columns, the normalized Laplacian matrix is calculated as follows:

$$\mathbf{L}_r = \mathbf{D}_r^{-1/2}(\mathbf{D}_r - \mathbf{W}_r)\mathbf{D}_r^{-1/2}, \tag{7}$$

$$\mathbf{L}_c = \mathbf{D}_c^{-1/2}(\mathbf{D}_c - \mathbf{W}_c)\mathbf{D}_c^{-1/2}. \tag{8}$$

Where: $\mathbf{L}_r$, $\mathbf{L}_c$ are the row and column normalized Laplacian matrices; $\mathbf{D}_r$, $\mathbf{D}_c$ are the row and column degree matrices.

For the double normalized matrix $\mathbf{X}^T\mathbf{L}_r\mathbf{X} + \mathbf{X}\mathbf{L}_c\mathbf{X}^T$ perform eigenvalue decomposition and select the first s feature dimensions to form the low-dimensional feature space. In the low-dimensional space, the rows and columns are separately clustered using K-means, and the objective function minimizes the clustering discrepancy:

$$\min_{C_r, C_c} \sum_{i \in C_r, j \in C_c} \left\| X(i,j) - \mu_{C_r, C_c} \right\|^2 . \tag{9}$$

Where μ_{C_r, C_c} represents the center of the row and column clusters.

2) TYPICAL SCENARIO GENERATION METHOD FOR EHCMS

The specific steps for generating typical scenarios based on SJC are as follows:

Step 1: Data Preprocessing.

Organize five sets of data: photovoltaic output, electricity demand, thermal demand, gas demand, and hydrogen demand, each containing time series data for 8760 hours across one year. Perform min-max normalization on each set of data to eliminate dimensional differences, ensuring that each variable's value is within the range of $[0, 1]$:

$$X' = \frac{X - X_{\min}}{X_{\max} - X_{\min}} . \tag{10}$$

Where X' represents the normalized data, and $X_{\max}$, $X_{\min}$ are the maximum and minimum values of each data set, respectively. Matrix reconstruction is then performed, transforming the original 3D data $\mathbf{X} \in \mathbb{R}^{365\times24\times5}$ into a 2D matrix $\mathbf{X} \in \mathbb{R}^{365\times120}$, where each row represents the multivariable time series feature for a single day.

Step 2: Spectral Joint Clustering.

Set the target number of clusters s, construct the similarity matrix, and compute the normalized Laplacian matrix. Perform singular value decomposition (SVD) and select the top s eigenvectors to form the low-dimensional feature space. K-means clustering is applied to the feature space to obtain the optimal number of clusters for rows k_r and columns k_c.

Step 3: Typical Day Extraction.

For each row cluster C_k, calculate the multivariate time series mean of all days contained in it, and use this as the typical day:

$$S_k^{(v)}(h) = \frac{1}{|C_k|} \sum_{d \in C_k} x^{(d,h,v)}, \quad h = 1, \ldots, 24; \; v = 1, \ldots, 5. \tag{11}$$

The probability of each typical day is computed based on the sample proportion within the cluster:

$$p_k = \frac{|C_k|}{365} . \tag{12}$$

Based on the selected typical days, extract the corresponding photovoltaic output, electricity demand, thermal demand, gas demand, and hydrogen demand data. Output s typical day datasets. Each typical day retains the full 24-hour photovoltaic output data and the coupling features of electricity, heat, and hydrogen loads, representing a similar daily scenario pattern within the dataset.

The algorithm flowchart for generating typical days based on spectral joint clustering is shown below.

III. LONG-TERM LOW-CARBON ECONOMIC DISPATCH MODEL FOR EHCMS

A. LONG-DURATION HYDROGEN STORAGE OPERATION MODEL

Between two consecutive operational days, the initial hydrogen storage mass in the hydrogen storage tank must satisfy the following:

$$\begin{aligned} S_{\mathrm{H2S},0}(r+1) = (1 - \sigma_{\mathrm{H2S}} \times 24) S_{\mathrm{H2S},0}(r) \\ + \Delta S_{\mathrm{H2S}}\big(k = h(r), 24\big). \end{aligned} \tag{13}$$

Where $S_{\mathrm{H2S},0}(r+1)$ represents the initial hydrogen storage mass in the tank on the $r+1$-th operational day, $h(r)$ is the mapping function between the typical day k and the operational day r.

To ensure that the total hydrogen storage amount in the tank is the same throughout the year, the following condition must be met:

$$\begin{aligned} S_{\mathrm{H2S},0}(1) = (1 - \sigma_{\mathrm{H2S}} \times 24) S_{\mathrm{H2S},0}(N_r) \\ + \Delta S_{\mathrm{H2S}}\big(k = h(N_r), 24\big). \end{aligned} \tag{14}$$

Where N_r represents the total number of operational days in the year.

The actual hydrogen mass in the tank at any moment during the year can be decomposed into the initial storage amount and the dynamic addition from typical day scenarios:

$$S_{\mathrm{H2S}}(r,t) = S_{\mathrm{H2S},0}(r) + \Delta S_{\mathrm{H2S}}\big(k = h(r), t\big). \tag{15}$$

Where $S_{\mathrm{H2S}}(r,t)$ represents the actual hydrogen mass stored in the tank on day r at time t hours, which is the sum of the initial hydrogen storage for day r and the hydrogen mass stored at time t on that day.

To ensure safe hydrogen storage operation, the hydrogen mass in the tank must meet the upper and lower limits:

$$\alpha_{\mathrm{H2S,min}} S_{\mathrm{H2S,cap}} \le S_{\mathrm{H2S}}(r,t) \le \alpha_{\mathrm{H2S,max}} S_{\mathrm{H2S,cap}} . \tag{16}$$

Since the above equation holds for each moment within the scheduling period, to reduce constraints, we simplify it as follows:

$$\begin{cases} \Delta S_{\mathrm{H2S,max}}(k) \ge \Delta S_{\mathrm{H2S}}(k,t), \\ \Delta S_{\mathrm{H2S,min}}(k) \le \Delta S_{\mathrm{H2S}}(k,t). \end{cases} \tag{17}$$

$$\begin{cases} S_{\mathrm{H2S},0}(r) + \Delta S_{\mathrm{H2S,max}}\big(k = h(r)\big) \le \alpha_{\mathrm{H2S,max}} S_{\mathrm{H2S,cap}}, \\ S_{\mathrm{H2S},0}(r) + \Delta S_{\mathrm{H2S,min}}\big(k = h(r)\big) \ge \alpha_{\mathrm{H2S,min}} S_{\mathrm{H2S,cap}}. \end{cases} \tag{18}$$

Where $\Delta S_{\mathrm{H2S,max}}(k)$ and $\Delta S_{\mathrm{H2S,min}}(k)$ represent the maximum and minimum hydrogen mass stored in the hydrogen tank on the k-th typical day, respectively, in kg.

B. LONG-TERM LOW-CARBON ECONOMIC DISPATCH OBJECTIVE FUNCTION FOR EHCMS

The long-term optimization operation model for EHCMs aims to minimize the system's total annual operating cost C, which includes the system's annual operation and maintenance cost C_{om}, energy purchasing cost C_{buy}, carbon trading cost C_{CO2}, waste treatment subsidy C_{waste}, and energy sales revenue C_{sell}. The objective is expressed as:

$$\min C = C_{\mathrm{om}} + C_{\mathrm{buy}} + C_{\mathrm{CO2}} - C_{\mathrm{sell}} . \tag{19}$$

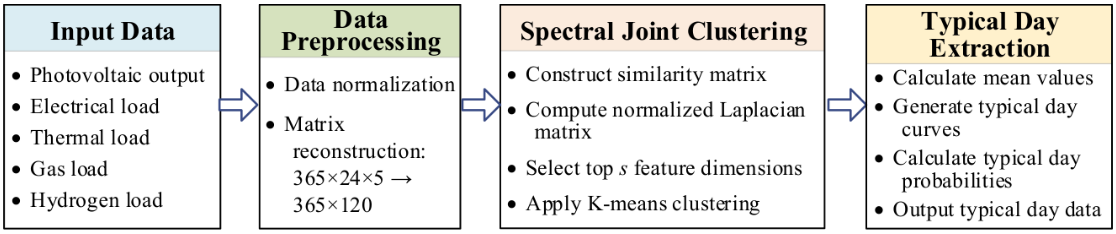

FIGURE 1. Flowchart for Generating Typical Scenarios Based on SJC

The operation and maintenance cost C_{om} refers to the total operation and maintenance costs of all equipment in the scheduling period. The expression is:

$$C_{\mathrm{om}} = \sum_{r=1}^{365}\sum_{t=1}^{24}\sum_{i}^{X} \lambda_i P_i(r,t)\Delta t. \tag{20}$$

Where λ_i is the unit capacity operation and maintenance cost for equipment i, $P_i(r,t)$ is the output power of equipment i at time t on operational day r, X represents the set of equipment in the system, including photovoltaic units, waste power generation, biogas fermentation, electrolyzers, hydrogen fuel cells, cogeneration units, electric boilers, energy storage batteries, thermal storage tanks, and hydrogen storage tanks.

The formula can be simplified using the mapping function $h(r)$ between the typical day k and the operational day r:

$$C_{\mathrm{om}} = \sum_{k=1}^{s}\sum_{t=1}^{24}\sum_{i}^{X} N_r p_k \lambda_i P_i(k,t)\Delta t. \tag{21}$$

Where p_k is the probability of typical day k occurring in the year, N_r is the total number of operational days in the year. The energy purchasing cost C_{buy} refers to the cost of purchasing energy from the upper-level grid. The expression is:

$$C_{\mathrm{buy}} = \sum_{r=1}^{365}\sum_{t=1}^{24} \left(c_e(t)P_{\mathrm{buy}}(r,t)\Delta t + c_g G_{\mathrm{buy}}(r,t)\Delta t\right) \tag{22}$$

Where $P_{\mathrm{buy}}(r,t)$ and $G_{\mathrm{buy}}(r,t)$ represent the purchased electricity power and natural gas power at time t on operational day r, respectively.

The waste treatment subsidy C_{waste} refers to the subsidy the system receives for processing rural waste. The expression is:

$$C_{\mathrm{waste}} = c_{\mathrm{waste}} \sum_{k=1}^{s}\sum_{t=1}^{24}\sum_{i}^{X} N_r p_k \left(W_{\mathrm{gar}}(k,t)\Delta t + M_{\mathrm{BD}}(k,t)\Delta t\right) \tag{23}$$

Where $W_{\mathrm{gar}}(r,t)$ is the amount of waste processed at time t on operational day r, $M_{\mathrm{BD}}(r,t)$ is the amount of organic waste input into the biogas tank at time t on operational day r.

The energy sales revenue C_{sell} refers to the revenue generated by the system from hydrogen sales. The expression is:

$$C_{\mathrm{sell}} = \sum_{k=1}^{s}\sum_{t=1}^{24}\sum_{i}^{X} N_r p_k c_{\mathrm{sell}} m_{\mathrm{sell}}(k,t)\Delta t. \tag{24}$$

C. LONG-TERM LOW-CARBON ECONOMIC DISPATCH CONSTRAINTS FOR EHCMS

1) ELECTRICAL POWER BALANCE CONSTRAINT

$$\begin{aligned} &P_{\mathrm{buy}}(r,t) + P_{\mathrm{PV}}(r,t) + P_{\mathrm{gar}}(r,t) \\ &\quad + P_{\mathrm{FC}}(r,t) + P_{\mathrm{CHP}}(r,t) + P_{\mathrm{ES,dis}}(r,t) \\ &\quad = P_{\mathrm{EL}}(r,t) + P_{\mathrm{EB}}(r,t) + P_{\mathrm{ES,ch}}(r,t) + P_L(r,t). \end{aligned} \tag{25}$$

Where $P_L(r,t)$ represents the electrical load of the system during time t of operational day r.

2) THERMAL POWER BALANCE CONSTRAINT

$$\begin{aligned} &H_{\mathrm{gar}}(r,t) + H_{\mathrm{CHP}}(r,t) + H_{\mathrm{EL}}(r,t) \\ &\quad + H_{\mathrm{FC}}(r,t) + H_{\mathrm{EB}}(r,t) + H_{\mathrm{HS,dis}}(r,t) \\ &\quad = H_{\mathrm{BD}}(r,t) + H_{\mathrm{HS,ch}}(r,t) + H_L(r,t). \end{aligned} \tag{26}$$

Where $H_L(r,t)$ represents the thermal load of the system during time t of operational day r.

3) NATURAL GAS BALANCE CONSTRAINT

$$G_{\mathrm{buy}}(r,t) + G_{\mathrm{BD}}(r,t) = G_{\mathrm{CHP}}(r,t) + G_L(r,t). \tag{27}$$

Where $G_L(r,t)$ represents the gas load of the system during time t of operational day r.

4) HYDROGEN ENERGY BALANCE CONSTRAINT

$$\begin{aligned} m_{\mathrm{EL}}(r,t) + m_{\mathrm{H2S,dis}}(r,t) &= m_{\mathrm{FC}}(r,t) + m_{\mathrm{sell}}(r,t) \\ &\quad + m_{\mathrm{H2S,ch}}(r,t) + m_L(r,t). \end{aligned} \tag{28}$$

Where $m_L(r,t)$ represents the hydrogen load of the system during time t of operational day r.

5) SYSTEM ENERGY PURCHASE CONSTRAINT

$$P_{\mathrm{buy,min}} \le P_{\mathrm{buy}}(t) \le P_{\mathrm{buy,max}}, \tag{29}$$

$$G_{\mathrm{buy,min}} \le G_{\mathrm{buy}}(r,t) \le G_{\mathrm{buy,max}}. \tag{30}$$

6) EQUIPMENT OUTPUT CONSTRAINTS

Equipment output in the EHCM is subject to the performance characteristics of the equipment and system requirements, typically constrained by upper and lower output limits and ramp-up constraints, expressed as:

$$P_{i,\min} \le P_i(r,t) \le P_{i,\max}, \tag{31}$$

$$R_{i,\mathrm{down}} \le P_i(r,t) - P_i(r,t-1) \le R_{i,\mathrm{up}}. \tag{32}$$

TABLE I. Time-of-use electricity pricing in Shanxi Province

Time Period	Time Interval	Electricity Price (¥/kWh)
Low Valley Period	00:00–08:00	0.395
Flat Period	12:00–17:00, 21:00–24:00	0.584
Peak Period	08:00–12:00, 17:00–21:00	0.790

7) ENERGY STORAGE DEVICE CONSTRAINTS

The power constraints for the energy storage battery and thermal storage tank are as follows:

$$S_{\mathrm{ES}}(t+1) = (1-\sigma_{\mathrm{ES}}\Delta t)S_{\mathrm{ES}}(t) + \left(\eta_{\mathrm{ES}}P_{\mathrm{ES,ch}}(t) - \frac{P_{\mathrm{ES,dis}}(t)}{\eta_{\mathrm{ES}}}\right)\Delta t. \tag{33}$$

$$\alpha_{\mathrm{ES,min}}S_{\mathrm{ES,cap}} \leq S_{\mathrm{ES}}(t) \leq \alpha_{\mathrm{ES,max}}S_{\mathrm{ES,cap}}. \tag{34}$$

For the thermal storage tank:

$$S_{\mathrm{HS}}(t+1) = (1-\sigma_{\mathrm{HS}}\Delta t)S_{\mathrm{HS}}(t) + \left(\eta_{\mathrm{HS}}H_{\mathrm{HS,ch}}(t) - \frac{H_{\mathrm{HS,dis}}(t)}{\eta_{\mathrm{HS}}}\right)\Delta t. \tag{35}$$

$$\alpha_{\mathrm{HS,min}}S_{\mathrm{HS,cap}} \leq S_{\mathrm{HS}}(t) \leq \alpha_{\mathrm{HS,max}}S_{\mathrm{HS,cap}}. \tag{36}$$

IV. CASE STUDY ANALYSIS

A. SYSTEM PARAMETER SETTINGS FOR EHCMS

To validate the effectiveness of the proposed model, a case study is conducted using data from a large-scale microgrid in Shanxi, China. The system and microgrid equipment parameters are shown in Tables 1 and 2. The simulation experiments are conducted in a Python 3.9.13 development environment, with a mathematical optimization model built using Pyomo 6.8.2. The Gurobi 12.0.1 solver is used for solving the model. All simulations are performed on a personal computer equipped with an Intel i7-9750H 2.6GHz CPU and 8GB RAM.

This paper uses the energy consumption simulation software EnergyPlus to generate the annual data for the system's electrical, thermal, gas, and hydrogen load demands, as well as photovoltaic output. Each variable is separately normalized using the min-max method to eliminate dimensional differences. The results after normalization are shown in Figure 2. The annual data is divided into 365 samples, with each sample containing 24 hours × 5 variables of time series data, forming a 3D matrix $\mathbf{X} \in \mathbb{R}^{365\times24\times5}$. The 3D data is then flattened into a 2D matrix $\mathbf{X} \in \mathbb{R}^{365\times120}$, where each row corresponds to the multivariate time series features of one day.

B. ANALYSIS OF TYPICAL DAY GENERATION RESULTS FOR EHCMS

Based on the Python open-source environment and utilizing the spectral co-clustering algorithm from the scikit-learn machine learning library, a joint clustering analysis is performed on the data matrix containing multi-dimensional time series data such as photovoltaic output, electrical/thermal/gas/hydrogen loads. The target number of clusters is set to $k = 12$, and the SpectralCoclustering class

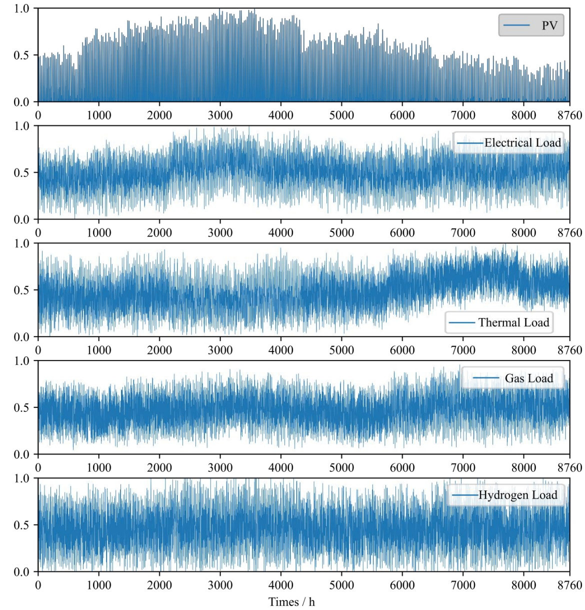

FIGURE 2. Normalized Annual Source-Load Data

from the sklearn.cluster module is used to build the clustering model. The fit method is used to perform synchronized co-partitioning on both the time and feature dimensions, resulting in clustering labels for each time point. The annual 8760 hours of operational data are ultimately categorized into 12 typical day scenarios, with each scenario fully retaining the original data's time correlation characteristics and multi-energy flow coupling features.

For each category, the Euclidean distance between the time series data of all days within the category and the category's mean is calculated. The day with the smallest distance is selected as the representative day for the category. The five-dimensional time series data of the representative day is then taken as the feature for that typical day. To reflect the frequency of each category's occurrence within the entire dataset, the typical day probability is assigned based on the proportion of days within each category, as shown in Table 3.

Using the spectral joint clustering method, 12 typical day source-load curves are obtained, and the normalized results are shown in Figure 3. The case study results demonstrate that the proposed method for generating typical days based on spectral joint clustering effectively addresses the computational complexity of clustering high-dimensional time series data through dimensionality reduction. This method provides data support for the efficient solution of the subsequent long-term energy system optimization model.

C. ANALYSIS OF LONG-TERM LOW-CARBON ECONOMIC DISPATCH RESULTS FOR EHCMS

This section first analyzes the variation in energy storage capacity under long-duration hydrogen storage characteristics and the system's long-term optimization under the tiered carbon trading mechanism. Figure 4 shows the variation curve of hydrogen storage mass in the hydrogen storage

TABLE II. Technical parameters of energy equipment

Equipment	Operating Cost	Maximum Capacity	Technical Parameters
Photovoltaic Unit	0.04 ¥/kWh	8000 kW	$k_{\mathrm{PV}} = -0.00485/^{\circ}\mathrm{C}$; $T_r = 25^{\circ}\mathrm{C}$
Waste Power Generation	0.07 ¥/kWh	5000 kW	$\eta_{\mathrm{WI}} = 0.35$; $\eta_{\mathrm{WG}} = 0.595$; $\eta_{\mathrm{WHB}} = 0.95$; $\eta_{\mathrm{aux}} = 0.25$
Biogas Fermentation	0.05 ¥/kWh	6000 kW	$\alpha_{\mathrm{BD}} = 0.4$; $\beta_{\mathrm{BD}} = 0.03$; $\eta_{\mathrm{B2G}} = 0.63$
Electrolyzer	0.10 ¥/kWh	5000 kW	$\eta_{\mathrm{EL,H2}} = 0.7$; $\eta_{\mathrm{EL,h}} = 0.9$
Fuel Cell	0.20 ¥/kWh	1000 kW	$\eta_{\mathrm{FC,e}} = 0.5$; $\eta_{\mathrm{FC,h}} = 0.3$
CCHP System	0.02 ¥/kWh	2000 kW	$\eta_{\mathrm{CHP}} = 0.35$; $\alpha_{\mathrm{CHP}} = 1.5$
Energy Storage Battery	0.08 ¥/kWh	10000 kWh	$\sigma_{\mathrm{ES}} = 0.01$; $\eta_{\mathrm{ES}} = 0.95$; $\alpha_{\mathrm{ES,min}} = 0.1$; $\alpha_{\mathrm{ES,max}} = 0.9$; $\beta_{\mathrm{ES,ch}} = 0.5$; $\beta_{\mathrm{ES,dis}} = 0.5$
Thermal Storage Tank	0.04 ¥/kWh	10000 kWh	$\sigma_{\mathrm{HS}} = 0.05$; $\eta_{\mathrm{HS}} = 0.9$; $\alpha_{\mathrm{HS,min}} = 0.1$; $\alpha_{\mathrm{HS,max}} = 0.9$; $\beta_{\mathrm{HS,ch}} = 0.2$; $\beta_{\mathrm{HS,dis}} = 0.2$
Hydrogen Storage Tank	0.02 ¥/kWh	14000 kWh	$\sigma_{\mathrm{H2S}} = 0.005$; $\eta_{\mathrm{H2S}} = 0.95$; $\alpha_{\mathrm{H2S,min}} = 0.1$; $\alpha_{\mathrm{H2S,max}} = 0.9$; $\beta_{\mathrm{H2S,ch}} = 0.1$; $\beta_{\mathrm{H2S,dis}} = 0.1$

TABLE III. Clustering results of typical days

Typical Day Group 1			Typical Day Group 2			Typical Day Group 3		
Day	Number of Days	Probability	Day	Number of Days	Probability	Day	Number of Days	Probability
1	24	6.58%	2	33	9.04%	3	28	7.67%
4	36	9.86%	5	25	6.85%	6	31	8.49%
7	29	7.95%	8	37	10.14%	9	32	8.77%
10	27	7.40%	11	30	8.22%	12	33	9.04%

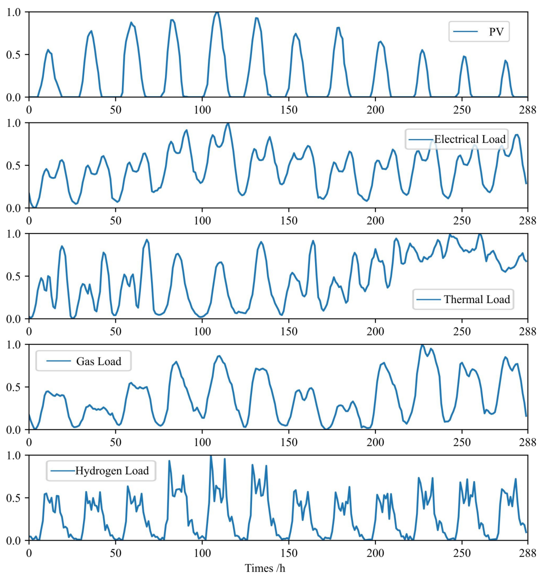

FIGURE 3. Normalized Typical Day Source-Load Data

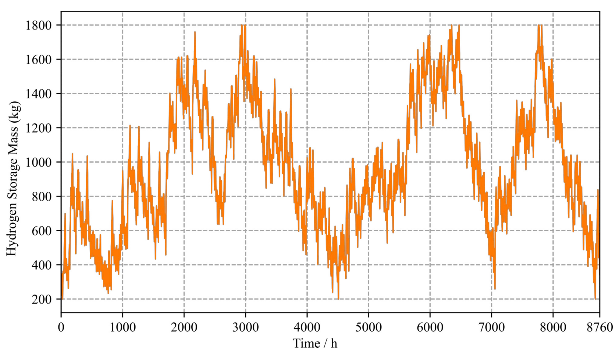

FIGURE 4. Variation Curve of Hydrogen Storage Tank Capacity

tank over the 8760 hours of the entire year.

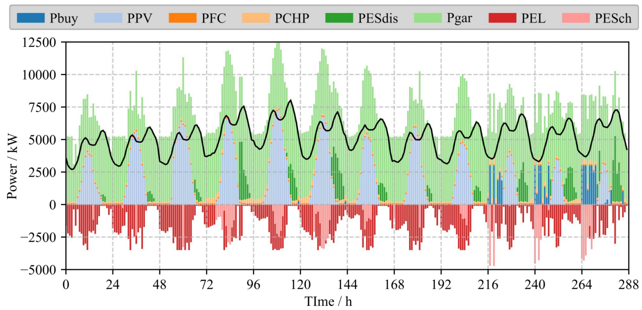

FIGURE 5. Electrical Power Balance Curve for 12 Typical Days

As shown in Fig. 4, when renewable energy generation is sufficient, the system uses electrolyzers to convert electrical energy into hydrogen for storage. During periods of insufficient energy supply, the system prioritizes using the hydrogen storage tank to supply energy, reducing the operation of high-carbon units. Under the incentive of the tiered carbon pricing mechanism, the microgrid's energy purchase cost is minimized at ¥8.32×10^5, with carbon emissions of only 8.07×10^6 kg, verifying that this model, through precise carbon constraints and inter-seasonal hydrogen energy dispatch, maximizes the adjustment ability of the hydrogen storage tank and achieves a balance between economic efficiency and low carbon emissions.

The results demonstrate that the proposed method simultaneously ensures the economic viability and low-carbon operation of EHCMs. This approach enables hydrogen storage tanks to efficiently absorb surplus solar power, while hydrogen fuel cells precisely respond to peak electricity demands, significantly reducing the EHCMs' external power procurement requirements. Electricity purchase costs are lowered to 6.53×10^5 yuan. Experimental results demonstrate a complementary relationship between energy storage batteries and hydrogen storage tanks, forming a short-to-long cycle synergy that jointly optimizes power scheduling at both intraday and cross-day scales. Excess midday electricity is prioritized for hydrogen production rather than battery charging, reducing battery degradation. During nighttime when solar output ceases, hydrogen stored in tanks continuously supplies the system, while batteries perform fine-tuning adjustments during load fluctuations. Constrained by tiered carbon trading mechanisms targeting high-carbon emissions, the system prioritized low-carbon

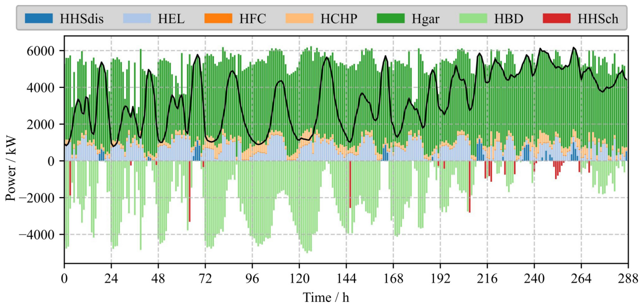

FIGURE 6. Thermal Power Balance Curve for 12 Typical Days

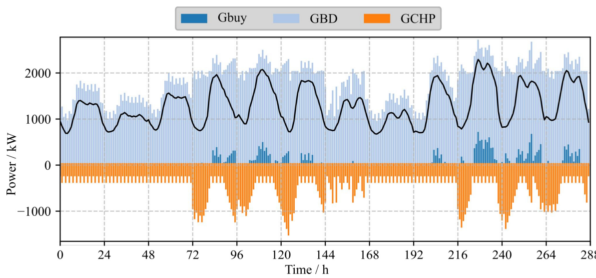

FIGURE 7. Gas Power Balance Curve for 12 Typical Days

energy sources like waste-to-energy and photovoltaics. This further reduced carbon emissions to 8.07×10^6 kg, with carbon trading costs of 2.10×10^6 yuan. Total costs decreased to 8.43×10^6 yuan, achieving a favorable balance between economic efficiency and low-carbon performance in power dispatch.

It is worth noting that the dispatch results also carry implications at the device level. The operating profiles of the electrolyzer and fuel cell obtained from the long-term optimization define the loading spectra of their power-electronic interfaces: frequent partial-load operation and start-stop cycles directly affect converter efficiency, harmonic injection, and the thermal stress of electromagnetic components. The typical-day operating envelopes extracted in this study can therefore serve as boundary conditions for the subsequent electromagnetic and electrothermal design of the conversion equipment, which is left for future work.

The method proposed in this paper combines the advantages of long-term hydrogen storage operation with a tiered carbon trading mechanism, fully utilizing waste-derived heat and residual heat from electrolyzer hydrogen production. During peak photovoltaic generation periods, electrolyzers operate at full capacity for hydrogen production, with substantial residual heat efficiently stored in thermal storage tanks. Hydrogen fuel cells and thermal storage tanks synergistically release heat to precisely match thermal loads. The heat supplied to the biogas digester becomes more stable, boosting biogas production. This optimized thermal energy scheduling reduces carbon emissions to 8.07×10^6 kg, achieving a favorable balance between economic efficiency and low-carbon performance in thermal energy management.

Under the proposed scheme, the tiered carbon pricing

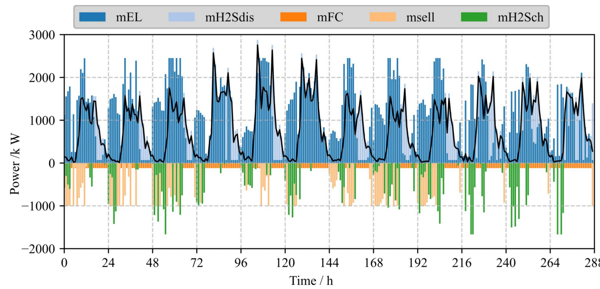

FIGURE 8. Hydrogen Power Balance Curve for 12 Typical Days

system prioritizes biogas utilization, with digester output precisely matched to gas demand. Hydrogen storage tanks accumulate hydrogen during midday photovoltaic surplus periods and release it for winter energy supply, enabling higher self-sufficiency rates. The gas procurement cost is 179,000 yuan, and the total energy procurement cost is only 832,000 yuan.

The tiered carbon pricing proposed in this paper drives the system to maximize renewable energy utilization. Electrolyzers fully absorb surplus electricity during peak photovoltaic generation periods, while hydrogen storage tanks precisely match hydrogen charging and discharging with hydrogen demand. Hydrogen sales volume is rationally output during periods of hydrogen surplus, generating revenue of 2.23×10^6 yuan, achieving a balance between economic viability and low-carbon performance. The proposed method enhances hydrogen self-sufficiency through efficient hydrogen regulation, reducing external energy procurement and carbon emissions. Hydrogen sales revenue and low-carbon subsidies cover additional operational costs, significantly improving the economic viability and low-carbon performance of hydrogen scheduling within the energy system.

V. CONCLUSION

This study has addressed the medium-to-long-term operational optimization of electro-hydrogen coupled microgrids (EHCMs) and proposed a low-carbon economic dispatch framework that incorporates long-duration hydrogen storage and a tiered carbon trading mechanism. The main findings are as follows:

(1) The proposed typical-day generation method based on spectral joint clustering effectively extracts 12 representative daily scenarios from 8760 hours of multi-energy data. By clustering the temporal and feature dimensions simultaneously through eigen-decomposition of normalized Laplacian operators, the method retains the spatiotemporal correlations and multi-energy coupling characteristics of the original data while reducing the computational burden of the long-term optimization to a tractable level.

(2) The long-duration hydrogen storage operation model, which decomposes the annual hydrogen inventory into an inter-day initial storage trajectory and intra-day dynamic increments, guarantees the state continuity of the hydrogen storage tank across the whole year through intraday-continuity and interday-linkage con-

straints, and simplifies the hourly capacity constraints into typical-day extreme-value constraints without loss of feasibility.

(3) Case studies of a large-scale microgrid in Shanxi, China, demonstrate that the synergy between long-duration hydrogen storage and the tiered carbon trading mechanism effectively reduces the annual energy purchase cost, carbon emissions, and the total annual cost while maintaining the coordinated balance among electricity, heat, gas, and hydrogen supply.

Beyond system-level economics, the significance of these results is twofold. Practically, the proposed framework provides rural and park-level EHCMs with a computationally tractable tool for annual operation planning under carbon market constraints. Scientifically, the extracted typical-day operating envelopes and loading spectra of electrolyzers, fuel cells, and their power-electronic interfaces constitute quantitative boundary conditions for the electromagnetic and electrothermal design of these energy conversion devices, and the spectral joint clustering method demonstrates how eigen-analysis techniques familiar to the computational electromagnetics community can be transferred to high-dimensional energy data analysis. Future work will couple the dispatch model with device-level electromagnetic-thermal models of the conversion equipment and extend the framework to distribution networks with multiple interconnected EHCMs.

ACKNOWLEDGMENT

This work was supported by the Science and Technology Project of State Grid Jiangsu Electric Power Company ("Key Technology Research on Flexible Configuration and Coordinated Control of Multi-Scenario Electric-Hydrogen Coupled Energy Systems", No. J2024187).

REFERENCES

[1] M. Laimon and T. Yusaf, "Towards energy freedom: Exploring sustainable solutions for energy independence and self-sufficiency using integrated renewable energy-driven hydrogen system," *Renew. Energy*, vol. 222, Art. no. 119948, Feb. 2024. DOI: 10.1016/j.renene.2024.119948.

[2] J. Park, S. Kang, S. Kim, H. Kim, S.-K. Kim, and J. H. Lee, "Optimizing green hydrogen systems: Balancing economic viability and reliability in the face of supply-demand volatility," *Appl. Energy*, vol. 368, Art. no. 123492, Aug. 2024. DOI: 10.1016/j.apenergy.2024.123492.

[3] G. Pan, W. Gu, Y. Lu, H. Qiu, S. Lu, and S. Yao, "Optimal planning for electricity-hydrogen integrated energy system considering power to hydrogen and heat and seasonal storage," *IEEE Trans. Sustain. Energy*, vol. 11, no. 4, pp. 2662–2676, Oct. 2020. DOI: 10.1109/TSTE.2020.2970078.

[4] S. S. Zehra, A. U. Rahman, and I. Ahmad, "Fuzzy-barrier sliding mode control of electric-hydrogen hybrid energy storage system in DC microgrid: Modelling, management and experimental investigation," *Energy*, vol. 239, Art. no. 122260, Jan. 2022. DOI: 10.1016/j.energy.2021.122260.

[5] L. Lin, K. Ou, Q. Lin, J. Xing, and Y.-X. Wang, "Two-stage multi-strategy decision-making framework for capacity configuration optimization of grid-connected PV/battery/hydrogen integrated energy system," *J. Energy Storage*, vol. 97, Art. no. 112862, Sep. 2024. DOI: 10.1016/j.est.2024.112862.

[6] J. Chen, H. Bie, J. Wang, and B. Sun, "Optimization operation method for hydrogen-compressed natural gas-integrated energy systems considering hydrogen-thermal multi-energy inertia," *Results Eng.*, vol. 25, Art. no. 103652, Mar. 2025. DOI: 10.1016/j.rineng.2024.103652.

[7] G. Wang, K. Verleysen, R. De Meulenaere, and J. Blondeau, "Multi-objective optimization of hybrid energy storage systems under uncertainty," *J. Energy Storage*, vol. 111, Art. no. 115218, Mar. 2025. DOI: 10.1016/j.est.2024.115218.

[8] A. Miao, Y. Yuan, Y. Huang, H. Wu, and C. Feng, "Stochastic optimization model of capacity configuration for integrated energy production system considering source-load uncertainty," *Sustainability*, vol. 15, no. 19, Art. no. 14247, Sep. 2023. DOI: 10.3390/su151914247.

[9] Z. Xu, F. Chen, X. Yang, and Q. Lu, "Optimal configuration of hybrid energy storage capacity in a grid-connected microgrid considering laddering carbon trading and demand response," *Energies*, vol. 17, no. 1, Art. no. 139, Jan. 2024. DOI: 10.3390/en17010139.

[10] M. M. Kamal, I. Ashraf, and E. Fernandez, "Optimal sizing of standalone rural microgrid for sustainable electrification with renewable energy resources," *Sustain. Cities Soc.*, vol. 88, Art. no. 104298, Jan. 2023. DOI: 10.1016/j.scs.2022.104298.

[11] C. Li et al., "Optimal planning of islanded integrated energy system with solar-biogas energy supply," *IEEE Trans. Sustain. Energy*, vol. 11, no. 4, pp. 2437–2448, Oct. 2020. DOI: 10.1109/TSTE.2019.2958562.

[12] X. Fu and Y. Zhou, "Collaborative optimization of PV greenhouses and clean energy systems in rural areas," *IEEE Trans. Sustain. Energy*, vol. 14, no. 1, pp. 642–656, Jan. 2023. DOI: 10.1109/TSTE.2022.3223684.

[13] H. Tan, Z. Li, Q. Wang, and M. A. Mohamed, "A novel forecast scenario-based robust energy management method for integrated rural energy systems with greenhouses," *Appl. Energy*, vol. 330, Art. no. 120343, Jan. 2023. DOI: 10.1016/j.apenergy.2022.120343.

[14] M. Sharifzadeh, N. Cooper, H. van't Noordende, and N. Shah, "Operational strategies and integrated design for producing green hydrogen from wind electricity," *Int. J. Hydrogen Energy*, vol. 64, pp. 650–675, Apr. 2024. DOI: 10.1016/j.ijhydene.2024.03.237.

[15] Y. Wang, Y. Qin, Z. Ma, Y. Wang, and Y. Li, "Operation optimisation of integrated energy systems based on cooperative game with hydrogen energy storage systems," *Int. J. Hydrogen Energy*, vol. 48, no. 95, pp. 37335–37354, Dec. 2023. DOI: 10.1016/j.ijhydene.2023.06.170.

[16] W. Kong, K. Sun, and J. Zhao, "Two-stage optimal scheduling of community integrated energy system considering operation sequences of hydrogen energy storage systems," *J. Mod. Power Syst. Clean Energy*, vol. 13, no. 1, pp. 276–288, Jan. 2025. DOI: 10.35833/MPCE.2023.001027.

[17] A. Yu, Z. Li, and P. Liu, "Rural integrated energy system based on bibliometric analysis: A review of recent progress," *Processes*, vol. 12, no. 1, Art. no. 176, Jan. 2024. DOI: 10.3390/pr12010176.

[18] A. Cai et al., "Double-layer cycle capacity optimization model of rural biogas-solar-wind integrated energy system," in *Proc. 4th Int. Conf. Smart Power Internet Energy Syst. (SPIES)*, Beijing, China, Dec. 2022, pp. 1648–1654. DOI: 10.1109/SPIES55999.2022.10082132.

[19] C. Wu, "Carbon emission evaluation and low carbon economy optimization scheduling of rural integrated energy system based on LCA method," *IEEE Access*, vol. 13, pp. 17182–17194, Jan. 2025. DOI: 10.1109/ACCESS.2025.3533099.

[20] X. Liu et al., "Two-layer optimal scheduling of integrated electric-hydrogen energy system with seasonal energy storage," *Int. J. Hydrogen Energy*, vol. 82, pp. 1131–1145, Sep. 2024.

[21] W. Li, M. He, and T. Cai, "Low-carbon economic dispatch of hydrogen-containing integrated energy system considering stepped demand response," *Energy Rep.*, vol. 11, pp. 4222–4232, Jun. 2024. DOI: 10.1016/j.egyr.2024.04.008.

[22] Z. Ji, H. Zhang, and P. Wang, "Model predictive control scheduling strategy for hydrogen-doped integrated energy system considering ladder carbon trading," *J. Therm. Sci.*, vol. 34, no. 2, pp. 337–351, Mar. 2025. DOI: 10.1007/s11630-024-2075-0.

[23] D. Lim, J. Cha, C. Seo, and G. Jang, "A two-layer robust model predictive control-based energy management system for a zero-carbon DC microgrid with hybrid hydrogen-battery energy storage," *Int. J. Electr. Power Energy Syst.*, vol. 174, Art. no. 111516, Jan. 2026.

[24] J. Chen and B. Sun, "Modeling and operation optimization of a hydrogen-compressed natural gas-integrated energy system with variable hydrogen content and flexible thermal load," *Energy Sci. Eng.*, vol. 13, no. 4, pp. 1858–1870, Apr. 2025.

[25] X. Li, L. Zhang, R. Wang, B. Sun, and W. Xie, "Two-stage robust optimization model for capacity configuration of biogas-solar-wind integrated energy system," *IEEE Trans. Ind. Appl.*, vol. 59, no. 1, pp. 662–675, Jan. 2023. DOI: 10.1109/TIA.2022.3217229.

[26] X. Sun, X. Cao, M. Li, Q. Zhai, and X. Guan, "Seasonal operation planning of hydrogen-enabled multi-energy microgrids through multistage stochastic programming," *J. Energy Storage*, vol. 85, Art. no. 111125, Apr. 2024. DOI: 10.1016/j.est.2024.111125.

[27] Y. Wu, Y. Wu, H. Çimen, J. C. Vasquez, and J. M. Guerrero, "Towards collective energy community: Potential roles of microgrid and blockchain to go beyond P2P energy trading," *Appl. Energy*, vol. 314, Art. no. 119003, May 2022. DOI: 10.1016/j.apenergy.2022.119003.